STYRELSEN FÖR

VINTERSJÖFARTSFORSKNING

WINTER NAVIGATION RESEARCH BOARD

Research Report No 138

Hanyang Gong

AN OVERVIEW OF DEM-CFD COUPLING METHODS FOR SHIP PERFORMANCE IN FSICR CHANNEL

Finnish Transport and Communications Agency
Finnish Transport Infrastructure Agency
Finland

Swedish Maritime Administration
Swedish Transport Agency
Sweden

Talvimerenkulun tutkimusraportit — Winter Navigation Research Reports
ISSN 2342-4303
ISBN 978-952-425-024-5

FOREWORD

In this report no 138, the Winter Navigation Research Board presents the results of OreDCs - An overview of DEM-CFD coupling methods for ship performance in FSICR channel. Project goal was to review open-source DEM-CFD software solutions that are able to model FSICR channel simulations.

The Winter Navigation Research Board warmly thanks the author for this report.

Helsinki

April 2026

Ville Häyrynen

Finnish Transport and Communications Agency

Amund Lindberg

Swedish Maritime Administration

Helena Orädd

Finnish Transport Infrastructure Agency

Jonas Gustaffson

Swedish Transport Agency

Aker Arctic

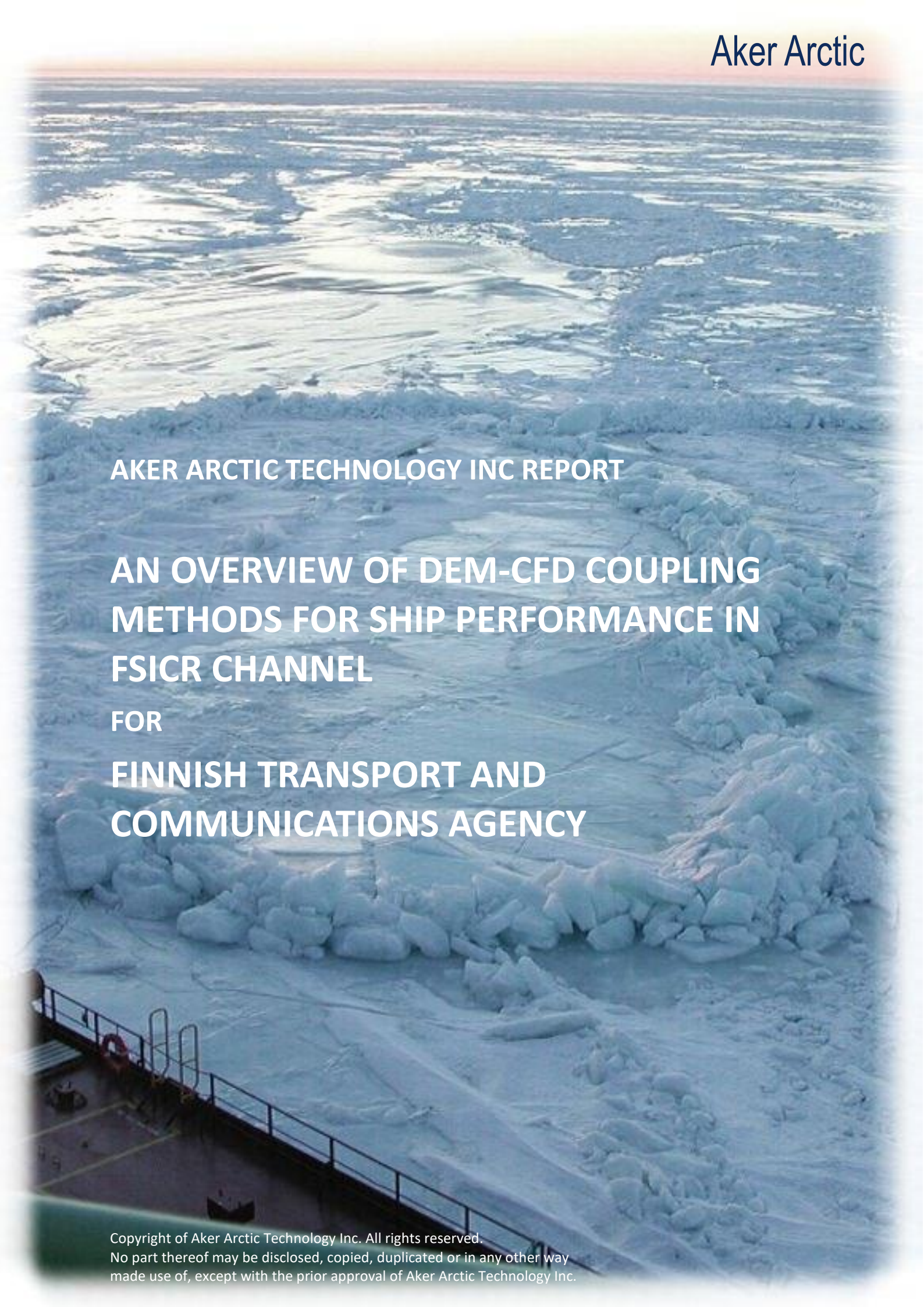

AKER ARCTIC TECHNOLOGY INC REPORT

AN OVERVIEW OF DEM-CFD COUPLING METHODS FOR SHIP PERFORMANCE IN FSICR CHANNEL

FOR

FINNISH TRANSPORT AND COMMUNICATIONS AGENCY

Name of document: K577_B - An overview of DEM-CFD coupling methods for ship performance in FSICR channel			
Document Responsible: Hanyang Gong		**Document Co-Author(s):** Malith Prasanna (VTT Technical Research Center of Finland)	
Document Reviewer: Riikka Matala		**Document Approver:** Maximilian Vocke	
Report number / Revision: K577 / B		**Status / Status Date:** Approved / 2025-11-25	
Client: Finnish Transport and Communications Agency / Ville Häyrynen			
Revision remarks: Small corrections according to Client's comments.			

Summary:
Ice model testing is a standardized method used to assess the performance of merchant ships for the purpose of assigning ice class certification. Nevertheless, current ice model testing methods encounter limitations when evaluating ice performance at high speeds due to hydrodynamic effects. Moreover, model testing of modern vertical-stem bow shapes is challenging since the model ice with scaled-down strength does not model well the resistance induced by displacing the brash ice mass to sides. However, both these challenges can be potentially addressed by using numerical modeling.

The integrated discrete element method–computational fluid dynamics (DEM-CFD) simulation approach has demonstrated promising as a supportive tool for model testing, offering a more thorough assessment of ship performance within Rule channels. However, open-source DEM-CFD codes have not been used previously to simulate ship performance within Rule channels.

This report provides an overview of prior research on simulating ships in Rule channels using coupled DEM-CFD methods. It first reviews the theoretical background of DEM-CFD coupling methods that have been applied to simulate brash ice model tests. The report then describes available open-source DEM-CFD packages and includes a detailed assessment. The feasibility of using open-source code is considered by incorporating knowledge of the FSICR channel as criteria for developing an appropriate DEM and CFD solver platform. A framework is planned for development in the subsequent stage of research following this project.

Keywords:
Review; Open-source codes; CFD; DEM; Coupling; FSICR; Brash ice

Client reference: PA (31077) - Finnish Transport and Communications Agency - W25-6 OreDCs		**Project number:** 31077	**Language:** English
Pages, total: 25	**Attachments:**	**Distribution list:**	**Confidentiality:** Confidential

TABLE OF CONTENTS

LIST OF FIGURES

LIST OF TABLES

ABBREVIATIONS

CFD ..... Computational fluid dynamics
DEM ..... Discrete element method
FSICR ..... Finnish-Swedish Ice Class Rule

1 INTRODUCTION

The modern ice-going ship hull form development aims to balance the ship performance over the whole operational profile, both in open water and in ice, to meet new sustainability regulations. Open water optimized vertical-stem bow shapes of these hulls tend to displace brash ice mass to sides than submerging them into water causing thick pile-up layers at the bow. Thus, it is challenging to grant ice class to such hull form by using traditional Rule methods, such as ice model testing according to the Finnish-Swedish Ice Rules (FSICR). Ice model testing typically applies Froude-Cauchy scaling while not scaling water viscosity, thus neglecting Reynolds similitude; an acceptable compromise at low speeds, where inertial and gravitational forces dominate over viscous effects. However, for high-speed tests or open-water optimized ice-going vessels, Reynolds similitude becomes important due to increased impact of viscous forces near the surface. Moreover, traditional methods that separately scale ice and hydrodynamic resistance may be inaccurate at high speeds because ice interacts with the fluid. Therefore, alternative methods are needed to better assess brash ice resistance in such contexts.

Numerical simulation tools offer an alternative for predicting ship performance in FSICR channels. Discrete element method (DEM) has been proved to be able to effectively simulate brash ice. Especially, recent studies on using solid ice cubes instead of model brash ice in tests has provided reliable resistance results, strengthening confidence in DEM's application for simulating ships in brash ice channels. Since hydrodynamics significantly affects the ship performance in brash ice channel for modern hull forms operating at higher speed, it requires fluid mechanics to be considered in the DEM simulations. At low speeds, simplified drag force could represent the fluid effect on brash ice behavior in DEM simulations. However, at higher speeds, it requires more advanced fluid mechanics, such as computational fluid dynamics (CFD) to be integrated in to DEM simulations. Coupled DEM-CFD simulation methods have been applied to simulate ships in brash ice channel and validated by the model testing since 2018 (Lu & Zou, 2018). However, these studies were set up on commercial simulation platform STAR-CCM+, which potentially limits the freedom of user modifications.

Therefore, this report aims to provide an overview of coupling methods for developing the framework of open-source DEM-CFD simulation platform. This could be then used to simulate a ship in FSICR brash ice channel with hydrodynamic effects at rule speed or higher in the future. This report first reviews the classic theory of DEM, CFD and the coupling methods used in the earlier publications on ships in brash ice channel. Next, the report examines the suitability of existing open-source DEM-CFD codes for this application. Finally, a simplified ship-brash ice application is presented to demonstrate the possibility of using one of the open-source codes to simulate ice-going ships in the FSICR channel.

2 OVERVIEW COUPLING DEM-CFD METHODS

This literature review covers scientific papers which used coupling methods of DEM-CFD to simulate an ice-going ship in brash ice channel. Applications using other numerical simulation methods, such as open dynamics engines, finite element method coupled with arbitrary Lagrangian Eulerian, and smoothed particle hydrodynamics, were reviewed in WNRB report 131.

The simulation scenario is defined as a ship moving at 5 kn in FSICR channel as represented by ice model testing. This includes brash ice, ship hull form, water, and air within rigid walls represented by the channel boundaries in the icy water. Water and air are modeled by CFD with Eulerian methods, while the ship hull is treated as a rigid boundary in both CFD and DEM domains. Ice blocks are modeled by DEM with Lagrangian method. Figure 1 presents a snapshot from a simulation of ship model in brash ice channel.

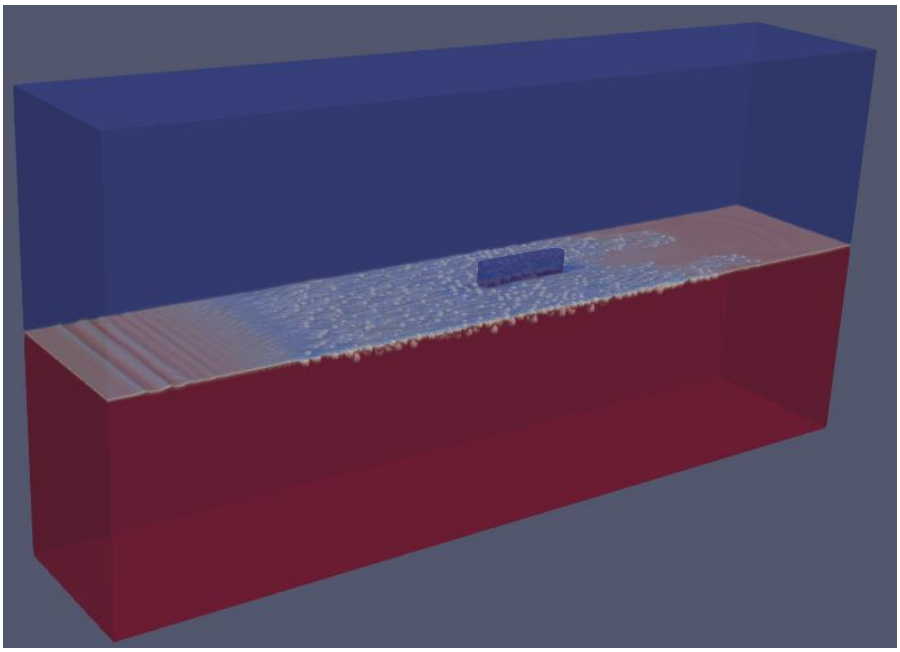

Figure 1: Snapshot from simulation of a dummy ship hull in brash ice channel

Since the most recent papers have used commercial software STAR-CCM+, the theory of DEM and CFD used there for coupling is reviewed below. It is noted that for both DEM and CFD, there are many other numerical theoretical equations available, but this review only focuses on the methods that have been tested already in the reviewed papers.

2.1 NUMERICAL APPROACH OF DEM-CFD

In particle-flow systems, CFD solvers typically divide computational domain into finite volumes or cells and use iterative methods to solve nonlinear flow equations. DEM is used to solve equation of motion of particles and requires an interface for integration with CFD solvers. Currently, there are three approaches available for coupling CFD solvers and DEM, based on the ratio of CFD cell size to particle diameter.

Based on the size ratio between the CFD finite volume cell and DEM element size, three DEM-CFD models are defined; unresolved DEM-CFD model if size ratio is over 3, resolved model if below 0.1, and semi-resolved DEM-CFD model for the size ratios in between.

In prior research, the unresolved DEM-CFD model was used in STAR-CCM+, as the DEM element sizes are smaller than the CFD cell size. Our recent work (Hanyang Gong & Malith Prasanna, 2025) used semi-resolved DEM-CFD model to test code reliability. It seems that the stability of the coupling scheme for modelling a ship in brash ice has not been investigated thoroughly. Therefore, in the following section, both the resolved and unresolved coupling schemes are reviewed in terms of calculation of the particle-fluid force which is the key in coupling method.

2.2 DEM

DEM is a widely applied particle-based method for simulating granular materials in both natural and industrial settings. DEM has been developed since 1979. Cundall & Otto DL Strack (1979) published the cornerstone paper of DEM for granular assemblies. Hopkins et al. (1991) and other pioneers applied DEM to simulate ice rubble in two dimensions and three dimensions. Since then, DEM has been widely applied in applications related to simulating ice rubble. A detailed review can be found in Tuhkuri & Polojärvi (2018). For example, smooth DEM has been developed as an in-house DEM tool by Aalto University Arctic Technology research group. Moreover, implicit, non-smooth and event-driven DEM simulations have been used by Rabatel M. et al. (2015) and van den Berg M. (2016). However, in these applications, only the drag force on particles was considered.

Since 2012, DEM-CFD method has been applied to simulating ice-ship interactions by E. Vroegrijk (2012; 2015) and, ice-structure interaction by Morgan (2015; 2016) and Yulmetov et al. (2017). Since 2018, commercial software packages with coupled CFD and DEM solvers have been applied to simulate ships in ice. Lu & Zou (2018) used EDEM and Fluent to simulate ships interacting with ice floes. After that, the main work flow turned to set up DEM-CFD simulations in commercial software STAR-CCM+. Therefore, the review below summarizes the theory used in the prior research in STAR-CCM+(SIEMENS Digital Industries, 2021).

In brash ice simulations, discrete elements represent brash ice blocks. The translational and rotational motions of every block is calculated through Newtonian dynamics using contact interactions, without relying on predefined failure models nor specific geometries for ice block arrangements. Equation of motion of a particle can be given as,

$$m\frac{dv}{dt} = F_c + F_{coh} + F_{pf} + mg \quad [1]$$

$$I\frac{d\omega}{dt} = T_c + T_f \quad [2]$$

where, t is time, m and I are mass and inertia tensors, respectively. v and ω are the linear and angular velocity of the particle, respectively. The right-hand side of the equations represents force and torque terms. F_c and F_{coh} are contact force and cohesion force, respectively. Brash ice is considered without cohesion, therefore $F_{coh} = 0$. mg is gravity. F_{pf} is the interaction force between fluid and the particle. T_c is contact torque and T_f is the

torque caused by fluid. A detailed calculation of torque can be found on the review paper by Ma et al. (2022a).

The ice blocks are influenced by several kind of forces, including contact forces, gravity, and water-related forces such as particle-fluid interaction forces utilized in CFD coupling or simplified drag forces in DEM simulations. Simplified drag force models generally offer sufficient accuracy for low-velocity conditions. Conversely, hydrodynamic forces, characterized by particle-fluid interaction forces, are better suited for high-velocity scenarios. Additional details regarding particle-fluid interaction forces can be found in Section 2.2.2.

2.2.1 CONTACT FORCE

In STAR-CCM+, a discrete element is described as a sphere. The contact force can be expressed as

$$F_c = F_n + F_t \quad [3]$$

where F_n is the normal force and F_t is tangential force.

The normal force F_n is expressed as

$$F_n = k_n \delta_n - \gamma_n \nu_n \quad [4]$$

where k_n is the normal spring stiffness and γ_n is the normal damping coefficient. δ_n is the normal overlap distance of two blocks, and ν_n is the normal component of the relative velocity of the two blocks.

The tangential force F_t is expressed as

$$F_t = \begin{cases} k_t \delta_t - \gamma_t \nu_t & (|k_t \delta_t| < |k_n \delta_n| c_f) \\ |k_n \delta_n| c_f \frac{\delta_t}{|\delta_t|} & (|k_t \delta_t| > |k_n \delta_n| c_f) \end{cases} \quad [5]$$

where k_t is the tangential spring stiffness and γ_t is the tangential damping coefficient. δ_t is the tangential overlap distance of two blocks, and ν_t is the tangential component of the relative velocity between two blocks, c_f is the friction coefficient between blocks.

Equations [3] - [5] express the basic contact force formulars. The coefficients such as spring stiffness, the overlap distance and the relative velocity vary depending on the contact models. Three contact models were tested by Zhang et al. (2022), which are Hertz-Mindlin contact model, linear spring contact model, and Walton Braun (WB) elastic-plastic contact model. Table 1 lists three contact models tested in Zhang et al. (2022).

Table 1: Three contact models tested in earlier research

Contact model	Spring coefficients	Damping coefficients	Overlap distance and relative velocity
Hertz-Mindlin (HM)	Equation [3] $k_n = \frac{4}{3}E_{eq}\sqrt{d_n R_{eq}}$ $k_t = 8G_{eq}\sqrt{d_n R_{eq}}$	$\gamma_n = \sqrt{5k_n M_{eq}}\gamma_{ndamp}$ $\gamma_t = \sqrt{5k_t M_{eq}}\gamma_{tdamp}$ $\gamma_{ndamp} = -\ln(c_{nrest}) / \sqrt{\pi^2 + \ln(c_{nrest})^2}$ $\gamma_{tdamp} = -\ln(c_{trest}) / \sqrt{\pi^2 + \ln(c_{trest})^2}$ $c_{nrest} = c_{trest} = 0.5$	$R_{eq} = \frac{1}{\frac{1}{R_i}+\frac{1}{R_j}}$ $M_{eq} = \frac{1}{\frac{1}{M_i}+\frac{1}{M_j}}$ $E_{eq} = \frac{1}{\frac{1-v_i^2}{E_i}+\frac{1-v_j^2}{E_j}}$ $G_{eq} = \frac{2(2-v_i)(1+v_i)}{E_i} + \frac{2(2-v_j)(1+v_j)}{E_j}$
Linear spring after Zhang et al. (2022)	Equation [3] $k_n = \frac{4}{3}E_{eq}\sqrt{d_n R_{eq}}$ $k_t = 8G_{eq}\sqrt{d_n R_{eq}}$	$\gamma_n = 2\gamma_{ndamp}\sqrt{k_n M_{eq}}$ $\gamma_t = 2\gamma_{tdamp}\sqrt{k_t M_{eq}}$ $\gamma_{ndamp} = \gamma_{ndamp} = 0.01$	
Walton Braun (WB) elastic-plastic model after Zhang et al. (2022)	Contact loading: $F_n = -k_1\delta_n$ $k_1 = -1.6\,\pi R Y_0$ $Y_0 = E \cdot YieldStressFraction$ Contact unloading: $F_n = -k_2(\delta - \delta_{def})$ $k_2 = k_1/E_f$ $\delta_{def} = \delta_{max}(1 - E_f)$		E is Young's modulus;$k_1$is post loading stiffness coefficient starting to lose contact; $k_2$is loading stiffness coefficient before contact separation; E_f is energy fraction to define the recovery of collision contact between blocks. δ_{max} is the maximum overlap during contact process

*R_{eq} is equivalent radius, M_{eq} is equivalent particle mass, E_{eq} is equivalent Young's modulus, G_{eq} is equivalent shear modulus. *M* is mass of sphere, v_i is Poisson's ratio.

Above equations are also valid if a DEM element is formed into a special shape by clumping many spheres by using equivalent radius, mass, Young's modulus and shear modulus. The tested DEM element shapes are sphere, cylinder, cube, tetrahedron, hexagon, and irregular polyhedron.

Figure 2 presents a few different DEM element shapes tested in earlier research.

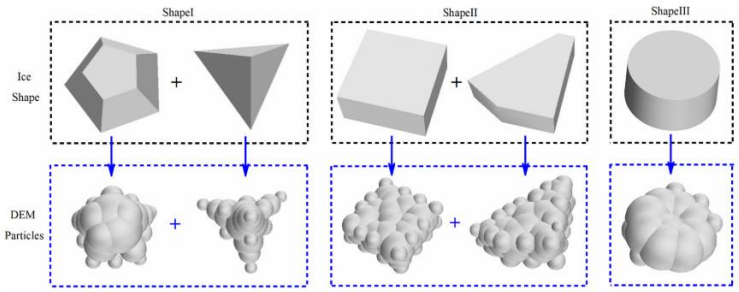

Fig. 12. Ice shape and DEM particles.

(a) After Zhang et al. (2022)

(b) After You et al. (2022)

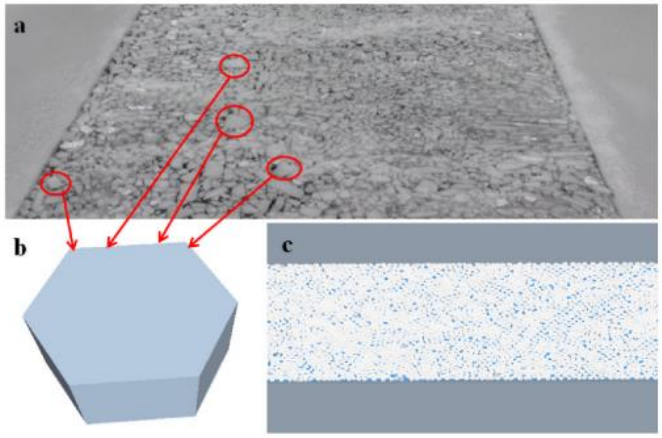

Fig. 9. The brash ice shape: (a) Brash ice distribution at HSVA; (b) Hexagonal brash ice model; (c) The channel arranged by hexagonal brash ice.

(c) After Xie et al. (2023).

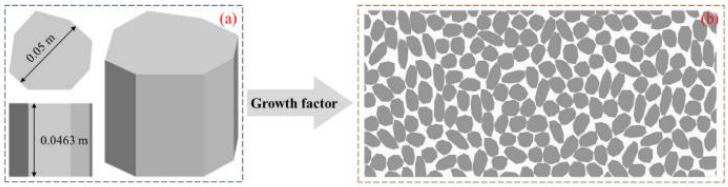

(d) After Zou et al. (2024).

Figure 2: Different DEM shapes composed of spheres tested in earlier research.

2.2.2 PARTICLE-FLUID INTERACTION FORCE

Equation [1] includes the coupling force, particle-fluid interaction force F_{pf}, which acts as a shared force transferring force between the CFD solver and DEM solver. In the unresolved DEM-CFD model, F_{pf} is expressed as

$$F_{pf} = \frac{1}{V_{cell}} \sum_{i=1}^{n_p} F_i \quad [6]$$

where V_{cell} is the volume of the CFD cell, F_i is the particle-fluid force on the DEM element i. F_i can be expressed as

$$F_i = F_d + F_b + F_l + F_a + F_p \quad [7]$$

where F_d is the drag force, F_b is the buoyance force (included in the pressure-gradient force), F_l is the lift force, F_a is the added mass force, and F_p is the pressure-gradient force of the fluid term acting on the DEM. The drag force F_d is typically the largest and normally only considered in the simulations. In some brash ice-ship simulations, lift force was not applied. The needs of lift force shall be investigated later. The sections below list the force formulas which have been recorded in the reviewed reference. For the resolved DEM-CFD model, void fraction is used to distribute the DEM force on the related CFD cells. This is further discussed in Section 2.4.

2.2.2.1 DRAG FORCE

One form of drag force F_d can be expressed as

$$F_d = \frac{\pi d_p^3 \beta (\boldsymbol{u}-\boldsymbol{v})}{6(1-\varepsilon)} \quad [8]$$

where d_p is the diameter of the volume equivalent sphere, β is the interphase exchange coefficient, u is the fluid speed. ε is the void fraction or volume fraction defined as the proportion of fluid accounted for the flow and pressure effects from the neighboring particles. For a loose granular system, $\varepsilon = 0$; for dense granular systems, $0 < \varepsilon < 1$. For non-spherical particles, drag force is more difficult to model accurately as both the irregular shape and the orientation can significantly affect the fluid field and particle-flow interaction. A coefficient can be introduced to correct the inaccuracy based on the drag force formula mentioned above. For more details, refer to Ma et al. (2022).

Most common form of drag force F_d is expressed as

$$F_d = 0.5 \rho_w c_d A_d v^2 \quad [9]$$

where ρ_w is the water density, A_d is the cross-section area of the particle, and v is the relative velocity between the fluid and the particle. c_d is the drag coefficient given by

$$c_d = \frac{24}{Re_p}\left(1 + AR e_p^B\right) + \frac{C}{(1+\frac{D}{Re_p})} \quad [10]$$

where Re_p is the Reynolds number of DEM elements, the rest A, B, C, and D are the coefficients of sphericity of DEM element. After Luo et al. (2020), $A = 8.1716\mathrm{e}^{-4.0665\phi}$,

$B = 0.0964 + 0.5565\phi$, $C = 76.69e^{-5.0746\phi}$, and $D = 5.378e^{-6.2122\phi}$. ϕ is particle sphericity. This form has been used in the STAR-CCM+ simulations. Compared to Equation [8], F_d does not consider the particle-flow interaction parameter ε.

2.2.2.2 PRESSURE GRADIENT FORCE AND BUOYANCE FORCE

Pressure gradient force is expressed as after Luo et al. (2020)

$$F_p = -V_p \nabla p_{static} \quad [11]$$

where V_p is the volume of DEM elements, ∇p_{static} is the gradient of static pressure in continuous phase. Pressure gradient force is typically considered as buoyancy governed by the Archimedes principle as $F_b = \rho_w g V$, where V is the particle's volume.

2.2.2.3 LIFT FORCE

Lift force is the mean force normal to the DEM element velocity. This force applies to the element moving relative to the fluid when the velocity gradient of fluid is orthogonal to the relative motion of the DEM element. Lift force is expressed after Luo et al. (2020),

$$F_l = 1.615 D^2 (\rho\mu)^{0.5} \left|\frac{\delta v}{\delta y}\right| v_s \quad [12]$$

where D is the DEM element diameter, ρ is the element density, μ is the dynamic viscosity, v is the fluid velocity, y is the velocity gradient direction, v_s is the slip velocity.

2.2.2.4 ADDED MASS FORCE

Added mass force is related to the fluctuation of particle velocity. In principle, added mass and added inertia are integrated in their equations of motion (Polojärvi, 2022). Added mass force can be also expressed as after Luo et al. (2020),

$$F_a = C_{vm} \rho V_p \left(\frac{Dv_s}{Dt} - \frac{dv_p}{dt}\right) \quad [13]$$

where C_{vm} is the added mass coefficient of the DEM element, V_p is the element volume, and ρ is fluid density, and v_p is the absolute velocity of the element.

2.3 CFD

Fluid mechanics is mathematically complex. The fluid described by Navier-Stokes equations could not be fully solved without simplifying the domain and assumptions using numerical methods, which refers to computational fluid dynamics (CFD). CFD solvers generally discretize the computational domains by finite volumes or cells and solve the nonlinear flow equations by using an iterative method. Finite volume method is selected among other computational fluid dynamics methods as it is easily formulated for handling meshes of complex geometries. For ship operations in brash ice channels, the fluid domain comprises of both air and water. The volume of fluid method is commonly employed to model two-phase fluids, whereas the potential flow method is used for ideal, inviscid, and irrotational single-phase flows.

Assuming the whole fluid domain is 1, the water phase fraction is $a_1 = 1$, the air is $a_1 = 0$ and a_1 on the water-air boundary is proportional in 0~1. The water and air are assumed to be incompressible fluids. In numerical modeling, the water and air interface tend to diffuse. An artificial compression term is added in the continuity equation to secure the sharpness of the phase interface.

Additionally, the void fraction is defined as $a_f = 1$ corresponds to fluid and $a_f = 0$ corresponds to solid (discrete elements). It is assumed that the DEM domain shares the same viscosity as the surrounding fluid. No specific calculations are performed within cells where the void fraction field has $a_f = 0$.

The continuity equation and momentum conservation equation are formulated as

$$\frac{\partial}{\partial t}(\varepsilon_f \rho_f) + \frac{\partial}{\partial x_j}(\varepsilon_f \rho_f u_j) = 0 \quad [14]$$

$$\frac{\partial}{\partial t}(\varepsilon_f \rho_f u_i) + \frac{\partial}{\partial x_j}(\varepsilon_f \rho_f u_j u_i) = -\frac{\partial p}{\partial x_i} + \frac{\partial}{\partial x_i}\left[\varepsilon_f u_f \left(\frac{\partial u_i}{\partial x_j} + \frac{\partial u_j}{\partial x_i}\right)\right] + F_{pf}. \quad [15]$$

The formular expression can be various depending on the assumptions. For example, the momentum conservation equation can be also expressed as after Luo et al. (2020), which is applied in the STAR-CCM+:

$$\frac{\partial}{\partial t}(\varepsilon_f \rho_f u_i) + \frac{\partial}{\partial x_j}(\varepsilon_f \rho_f u_j u_i) = -\varepsilon_f \frac{\partial p}{\partial x_i} - \frac{\partial}{\partial x_i}\left[\varepsilon_f u_f \left(\frac{\partial u_i}{\partial x_j} + \frac{\partial u_j}{\partial x_i}\right) + \frac{2}{3}\varepsilon_f u_f \frac{\partial}{\partial x_j}(u_j)\vec{\delta}\right] + \rho_f \varepsilon_f g - F_{pf} \quad [16]$$

where u is the fluid velocity, p is the fluid pressure, x denotes the coordinates, $\varepsilon_f = 1 - \varepsilon_p$ the volume fraction of the fluid term, ε_p is the volume fraction of the particle term, ρ_f is the fluid density, and F_{pf} is the source terms representing the forces due to particle and fluid interaction. The second term on the right-hand side of the momentum conservation equation is related to the stress tensor of the fluid $\overleftrightarrow{\tau_f}$. $\vec{\delta}$ is unit tensor.

In the numerical implementation, Newtonian fluid model is used. The turbulence model can solve Reynolds Averaged Navier-Stokes (RANS) equations where the statistical averaging is based on a proper time. The key approach is to decompose the flow variables into a time-mean value component and a fluctuating one, substituting in the original equations, and time-averaging the obtained equations (F. Moukalled et al., 2016).

2.4 COUPLING SCHEME

Depending on the simulation platform, the simulation program may begin with DEM, CFD, or both simultaneously. For instance, when starting with DEM, equations are used for DEM to provide particle information such as velocity and position within a fluid cell. This data is then input into the CFD solver, contributing to the right-hand side term of particle-fluid forces.

In unresolved DEM-CFD solvers, particle-fluid forces are calculated by summing the forces on particles and then dividing by the cell's volume to determine the average force on the

fluid cell. For the resolved DEM-CFD solver, forces on the DEM element calculated from the DEM solver are added to the fluid cell volume based on the void fraction a_f in the fluid cell.

The above-mentioned process can be considered as one-way coupling if the particle-fluid forces only be used once for one solver. For example, one-way coupling calculates fluid flow using CFD and its effect on the particles but does not account for the influence of particle motion on the fluid. Thus, interactions between ice particles and fluid are disregarded. Two-way coupling means that the fluid phase influences the ice particles, and the motion of the ice particles also impacts the fluid. Luo et al. (2020) indicated that two-way coupling can more effectively simulate brash ice behavior near the bow. For this reason, two-way coupling DEM-CFD is implemented. Although computational requirements increase, parallel computation enables the feasibility of establishing two-way coupling.

Figure 3 illustrates one possible two-way coupling DEM-CFD scheme. The solver begins by configuring the fluid parameters for CFD simulation and the particle properties for DEM simulation. The time step used in DEM solver is shorter than that of CFD. The DEM solver determines particle forces and moments using the initial position and velocity. In the CFD solver, the fluid domain is initialized to compute the phase fraction field (water and air phases) and void fraction field (solid and fluid), according to the initial CFD configuration. The fluid force, representing the particle-fluid interaction, is applied to the DEM particles. Following each DEM iteration, the updated velocities and positions of the DEM particles are utilized to map the void fraction and phase fraction within the fluid domain. The PISO algorithm is used to solve the turbulence model to obtain the converged fluid velocity and pressure after iterations. The first way of coupling is to integrate DEM particle velocity into the converged fluid velocity to form correct fluid velocity. The DEM particle velocity can be mapped to the CFD cells based on the void fraction field to get CFD cell velocity related to the DEM velocity. Using this velocity, the fluid velocity field at the solid and fluid interface can be updated based on the void fraction factor. For example, the corrected fluid velocity on a cell which is inside the DEM particle is the same as the DEM particle's velocity. Now the second way of coupling is initiated by using the corrected fluid velocity and converged fluid pressure to calculate the fluid force on the particle. Since the DEM particle is bigger than the CFD cell, the fluid force acting on the particle is the sum of the fluid forces of the CFD cells calculated by void fraction factor. This force is defined as the particle-fluid interaction force, which is delivered to the DEM solver to initiate the next round of calculations. The loop calculation continues until it reaches the end time (Gong & Prasanna, 2025).

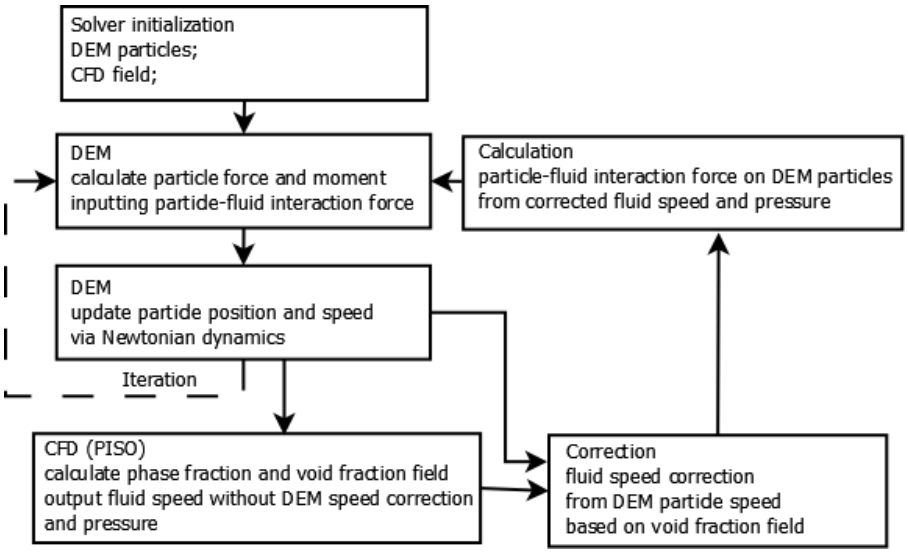

Figure 3: DEM-CFD coupling method calculation scheme, after Hanyang Gong & Prasanna (2025).

2.5 DISCUSSION OF APPLICATION TO FSICR CHANNEL

2.5.1 GEOMETRY AND SIZE DISTRIBUTION OF DISCRETE ELEMENTS

DEM elements can have different shapes: disc to (regular or irregular shape) polygon in two dimensions and sphere to polyhedron (convex or concave) in three dimensions. The DEM element shape determines the contact search algorithm and further influences the contact force modelling. The shape is important in determining the microscopic and macroscopic behavior of the granular material (Ma et al., 2022a). In ice research, 3D DEM simulations of ships navigating in ice floes (Polojärvi et al., 2021) indicated that the shape of ice floes is a significant factor influencing the magnitude of ice loads on vessels, in addition to ice thickness and size. Especially considering the interaction between the discrete elements and the fluid, the shape of the discrete elements would pronouncedly influence the overall behavior of the particle-flow system.

Some non-sphere elements have been applied to DEM simulations. Polygon ice blocks have been used in simulating ice rubble (Polojärvi, 2013), ridges (Gong, 2021), and ice floes (Polojärvi, 2022). However, these studies were limited to only DEM solvers. In DEM-CFD solvers, no real non-spherical polygon DEM elements have been used for simulating ships in brash ice channels. Some studies introduced so called isotropic and irregular polyhedral particles (Luo et al., 2020) and cylindrical particles (J. Voutilainen, 2023). In fact, it still belongs to the sphere-based particle model due to the calculation algorithm as described by Ma et al. (2022b). Particles of arbitrary shape are constructed from multiple spheres (termed sub-spheres) and are typically considered rigid. Conventional spherical contact detection algorithms identify contacts between sub-spheres. The cumulative forces and torques computed for each sub-sphere are then applied to the mass center of the constructed particle, allowing the simulation to achieve efficiency and robustness. Since these prior studies claim that the use of sphere-based polyhedral particles could provide relatively good results by considering computational efficiency and robustness, it is worth

testing the pure sphere simulations first with friction adjustment to compensate the shape effect on the results.

In addition, a realistic size distribution of brash ice in the channel should be considered in the simulations. Matala & Gong (2021) studied model-scale brash ice shape and size distribution from digital images from three ice sheets of model tests. This method may be used to acquire additional geometric information on brash ice in both model scale and full scale. Other full-scale information could also be considered in the simulation. Zhaka et al. (2024) presented macro-porosity and size distribution of the brash ice channel field data in the Bay of Bothnia, Luleå port, Sweden, during winters 2020-21 and 2021-22. Other full-scale data on ice block size in ridges can be found in Kulyakhtin & Høyland (2014).

2.5.2 SCALING OF MODEL SCALE SIMULATIONS

Validating simulations in relation to scale presents challenges. Direct validation using full-scale measurements can be difficult due to the possibility of incomplete data accumulation and the unpredictable nature of real environments. Consequently, simulation results may not be fully corroborated by full-scale measurements. As a result, attention often shifts to model scale or model testing, which is more controllable and easier to measure on a smaller scale. Simulation parameter values can be validated against model scale data; however, direct scaling up to full size may not yield accurate results. As previously noted, model testing cannot simultaneously satisfy both the Froude similitude and Reynolds similitude when fluid viscosity effects are significant. Therefore, phenomena observed at the model scale may not necessarily occur at full scale.

Therefore, utilizing simulation to support model testing demonstrates significant potential. Although direct validation of the simulation with full-scale data is not possible, simulation parameters associated with the Froude Law—once validated at model scale—can be directly scaled up to full scale. The fluid viscosity remains consistent between the model and full scale; however, the particle-fluid interaction force at model scale may differ from that at full scale. It is worth noting here that simulations are not limited by the physical properties of materials, thus it is possible to set up simulations fulfilling both Froude and Reynolds similitudes. Further research is required to investigate these topics.

2.5.3 FIXED MODEL OR FIXED ICE FIELD

In simulations, a fixed ship model is commonly used with brash ice and fluid is set to flow at a constant speed. The dynamic mesh technique can be applied to move the model in the brash ice channel to more closely reflect actual conditions. However, this approach requires updating the mesh at every time step, which significantly increases computational demands. As a result, the current practice follows previous research, such as Lu & Zou (2018), by utilizing a fixed ship model. Further investigation is recommended, for instance, to determine whether using either the fixed model or the stationary brash ice channel field affects total resistance results.

3 OPEN-SOURCE PACKAGES

3.1 OPEN-SOURCE SOFTWARE PACKAGE LIST

In this section we review several open-source DEM-CFD software packages with regard to simulating a brash ice model test. Source codes of all these packages are available to download free under some derivative of Open-Source software license. Then the code can be built by following the documentation. The code repositories also provide documentation and example simulation cases. Table 2 lists the software packages considered in this work and links to their repositories. The table also provides the relevant scientific publication which explains the underlying theoretical principles of the codes. It is worth noting here that this is not a full list of software packages available, rather a list compiled based on authors' knowledge.

Table 2: Open-source software packages reviewed

DEM-CFD package	Reference	Repository
CFDEM	(Kloss et al., 2012)	https://github.com/CFDEMproject/CFDEMcoupling-PUBLIC
YADE-OpenFOAM	Angelidakis et al., (2024)	https://gitlab.com/yade-dev/trunk
ESys-Foam	(Chen, 2009)	https://launchpad.net/esys-particle
openHFDIBDEM	(Kotouč Šourek et al., 2024)	https://github.com/techMathGroup/openHFDIB-DEM
PhasicFlowPlus	Norouzi, 2023)	https://github.com/PhasicFlow/PhasicFlowPlus
MFiX-DEM	(Syamlal et al., 1993)	https://mfix.netl.doe.gov/products/mfix/
KRATOS Multiphysics	(Dadvand et al., 2010)	https://github.com/KratosMultiphysics/Kratos
Lethe	(Blais et al., 2020)	https://github.com/chaos-polymtl/lethe
MigFlow	(Constant et al., 2019)	https://www.migflow.be/

A DEM-CFD software package generally consists of three major components, 1) DEM solver, 2) CFD solver and 3) DEM-CFD coupler. The DEM solver computes the motions of particles while the CFD solver computes the fluid flow. DEM-CFD coupler facilitates the communication between two solvers by transceiving fluid-particle interaction forces. In the majority of the opensource software packages reviewed here, DEM and CFD solvers come as two separate packages and the DEM-CFD coupler as a feature of DEM solver. Table 3 provides a summary of the composition of above-mentioned DEM-CFD packages.

Table 3: Summary of reviewed open-source DEM-CFD software package compositions

DEM-CFD software package	DEM solver	CFD solver	DEM-CFD coupler
CFDEM	LIGGGHTS	OpenFOAM	CFDEM
YADE-OpenFOAM	YADE	OpenFOAM	FoamCoupling
ESys-Foam	ESyS-Particle	OpenFOAM	esys-foam-dem
openHFDIB-DEM	openHFDIB-DEM	OpenFOAM	openHFDIB-DEM
PhasicFlowPlus	PhasicFlow	OpenFOAM	PhasicFlow
MFiX-DEM	MFiX-DEM	MFiX	MFiX-DEM
KRATOS Multiphysics	Kratos-DEM	Kratos	Kratos
Lethe	Lethe-DEM	Lethe	Lethe
MigFlow	LMGC90	MigFlow	MigFlow

In the table it is noticeable that OpenFoam seems to be the most widely used CFD solver in DEM-CFD software packages. This is because OpenFoam is highly customizable and used widely in both academia and in industry. Coupling DEM with OpenFoam follows the principles presented in Section 2. However, KRATOS, Lethe and Migflow are Finite Element Method (FEM) CFD solvers, thus governing equations behind coupling them with DEM are different. An overview of this method can be found in Blais et al. (2020)

3.2 COMPARISION OF FEATURES

As the first step of this review, we compare the different features of DEM-CFD software package. The features of interest here are free surface modeling, importing complex ship geometry, fully resolved hydrodynamics and polyhedral DEM elements. As illustrated in Figure 1, a brash ice ship model test consists of four physical regions: water, air, brash ice and ship model. Water and air constitute the continuum which ship model and ice are embedded at the free surface. Movement of the ship model creates waves in the water-air interface which in turn affects the movement of brash ice. Moreover, the shape of the ship model at bow affects the generated wave patterns. Thus, among the features listed above, free surface modeling and importing complex ship geometry are must have features for simulating a brash ice ship model test. Another key feature of a DEM-CFD solver is how fluid flow around particles is solved. In fully resolved methods fluid flow is solved by using an immersed boundary or fictitious domain method and requires finer CFD mesh with respect to particle size. Meanwhile, unresolved solvers use empirical models to compute fluid-particle forces, thus coarser meshes can be used with reduced computational costs. In case of simulating brash ice ship model tests, fully resolved methods provide higher accuracy at the expense of computational costs. It is worth noting here that unresolved methods are sufficiently accurate as well for the current application since ice particles do not have high relative velocities with respect to the fluid. Voutilainen, (2023) showed that the particle shape has significant effect on DEM-CFD simulation results of brash ice model test. Spherical particles seem to underestimate the resistance due to the lack of particle interlocking. Interlocking helps formation of particle clusters which in turn exert higher forces on ship model due to higher added mass and friction. Thus, polyhedral particles would be the ideal method for modeling brash ice. Nevertheless, lack of interlocking can be circumvented by using rolling friction when spherical particles are used. Table 4 summarizes and compares the above-mentioned features in open-source software packages reviewed.

Table 4: Comparison of features of reviewed open-source DEM-CFD software packages

DEM-CFD software package	Free surface modeling	Complex ship geometry	Fully resolved	Polyhedral particles
CFDEM	yes	yes	yes	no
YADE-OpenFOAM	no	yes	no	yes
ESys-Foam	no	yes	no	no
openHFDIB-DEM	no	yes	yes	yes
PhasicFlowPlus	yes	yes	yes	no
MFiX-DEM	no	no	no	no
KRATOS Multiphysics	no	no	no	yes
Lethe	yes	no	no	no
MigFlow	yes	no	no	no

As mentioned in the previous section OpenFOAM is the most widely used CFD solver in DEM-CFD packages. OpenFOAM consists of numerous sub-solvers tailored to solving Navier Stoles equations under different flow conditions. Among those, InterFoam is the solver of interest here which can solve two-phase, incompressible and immiscible flow using Volume of Fluid (VOF) method. Referring to the literature and documentation of above codes, we found that CFDEM has an implementation of coupling between LIGGGHTS and InterFOAM. Meanwhile, YADE, openFHDIB and EsysFoam are coupled with PimpleFOAM and IcoFoam respectively. Those are single phase flow solvers. PhasicFlowPlus also has an implementation of coupling between a VOF solver which can be used to solve two-phase flows. Lethe and MigFlow use particle finite element method to resolve free surface where nodes of the FEM mesh are displaced to follow the moving interface. OpenFoam has in-built utility feature snappyHexMesh to generate complex meshes. Thus, all DEM-CFD packages using OpenFOAM inherit this feature by default. The FEM based CFD solvers reviewed here do not have inbuilt complex meshing utilities, thus only support simple geometries.

3.3 POSSIBLE APPLICATIONS TO SIMULATING FSICR CHANNEL

Comparing software features against brash ice model test simulation requirements, it is apparent that CFDEM and PhasicFlowPlus are the possible candidates for the task. It is worth noting here that the authors did not find any example use cases of these software packages resembling brash ice model test. Thus, in this section we examine the literature related to these software packages where they have been used to simulate particle laden two-phase fluid flow.

CFDEM package seems to be the most widely used among the aforementioned, to model two-phase fluid flow with suspended particles. Su et al. (2025) used unresolved CFDEM solver to model dam-break wave impact on rock pile while Shen et al. (2022, 2024) have used resolved CFDEM solver to model the same. Li et al. (2025) developed a hybrid approach to combine both unresolved and resolved solvers to model particles with significant size differences. The method is then used to model particle sedimentation as well as dam-break. CFDEM opensource package currently supports only spherical particles, yet complex particle shapes can be replicated by clumping particles together (Shen et al.,

2024). PhasicFlowPlus is equipped with a fully resolved volume of fluid method solver that can be used to simulate two-phase flow with particles. GitHub repository of the package provides an example case for dam-break simulations (Hosseini & Joghataie, 2025), nevertheless there has not been any scientific publications related to this use.

4 EXAMPLE OF OPEN-SOURCE CODE APPLICATION

Based on the discussion in Chapters 3 and 4, the following example demonstrates an open-source code CFDEM's application on simulating a ship in the FSICR channel. In this example we use a semi-resolved DEM-CFD solver to simulate DEM particles that are larger than CFD cells. The ratio of DEM particle diameter to CFD cell size is approximately 4.5, which allows for a more accurate description of flow effects on ice blocks without incurring high computational costs from small CFD meshes. Parallel computation is used to decrease computational time.

This study case is a replication of Voutilainen (2023) STAR-CCM+ simulations of a dummy hull in FSICR channel. The simulation setup is illustrated in Figure 4. The simulation domain has *xyz* coordinate system: 10 m long, 2 m wide, 2.5 m of water depth and 2.5 m of air thickness. The diameter of the bow is 0.2 m in model scale with a total length of 1.2 m and thickness of 0.5 m. The velocity of the field is set to 0.74 m/s. Assuming the scaling factor is 100, the speed here in full scale is equivalent to 15 kn. Table 5 lists the simulation parameters.

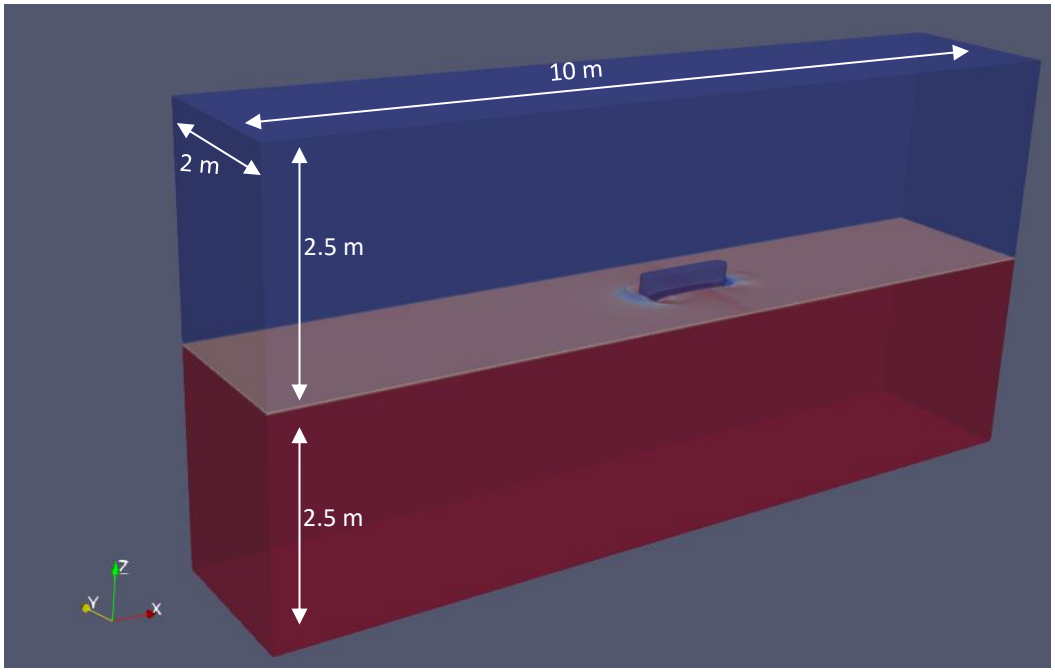

Figure 4: Simulation domain

Table 5: Simulation parameters

	Parameter	Value
DEM	Particle diameter [m]	0.1
	Young's modulus [Pa]	2.0e+9
	Poisson's ratio	0.3
	Ice-ice friction coefficient	0.3
	Ice-structure friction coefficient	0.1
	Ice density [kg/m^3]	920
	Flow velocity [m/s]	0.74
	Time step [s]	1.0e-5
CFD	Water density [kg/m^3]	1010
	Water kinematic viscosity [m^2/s]	1.0e-6
	Air density [kg/m^3]	1.2
	Air kinematic viscosity [m^2/s]	1.48e-5
	Cell size [m]	0.02
	Velocity [m/s]	0.74
	Time step [s]	1.0e-3

Figure 5 presents DEM-CFD simulation snapshot with color bar indicating v_x at 3.0 s. DEM elements are represented by the void fraction within the CFD domain and are also colored according to v_x from the CFD results. As both brash ice and the flow approach the dummy hull, a decrease in their velocities is observed. This reduction in brash ice velocity can be attributed to the drag force in the DEM simulation. Additionally, both brash ice and flow speeds are reduced due to the coupling loop calculation. Following the passage of brash ice past the dummy hull, the flow field velocity returns to the prescribed value. These observations contribute to the understanding of brash ice mechanics and associated hydrodynamic effects during high-speed interactions with a dummy ship hull. More analysis should be done after the model is validated in the future.

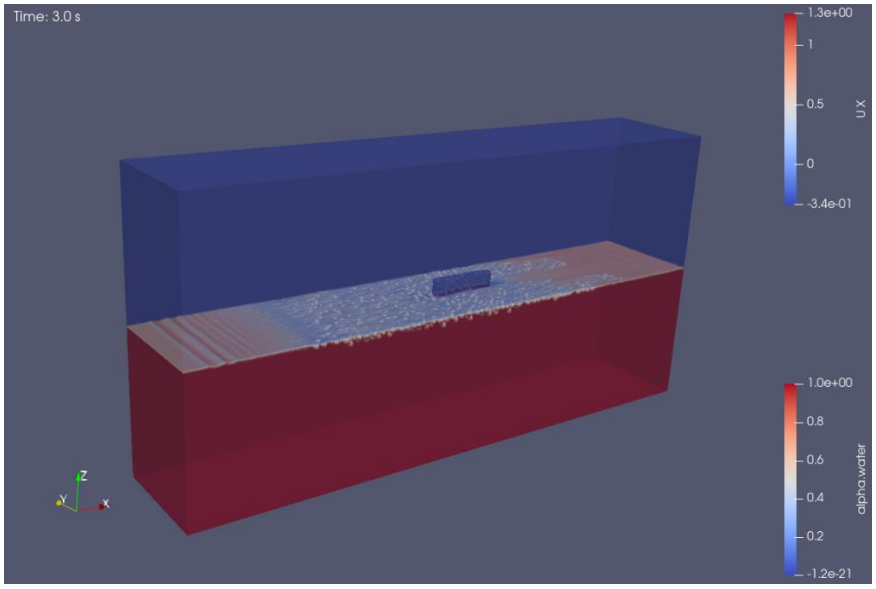

Figure 5: Simulation snapshot at 3.0 s

5 CONCLUSIONS

The present report reviewed the DEM-CFD coupling methods for the application of simulating a brash ice ship model test. The theoretical background related to DEM, CFD and coupled DEM-CFD was introduced and prior work related to the topic where commercial software platforms had been used was discussed. Then the available open-source software packages were reviewed for the application. It was found that the CFDEM and PhasicFlowPlus codes are the most suitable open-source packages available that can be used for simulating brash ice ship model tests. Finally, a demonstrative simulation of dummy hull in brash ice was performed by using CFDEM as a proof of concept of using open-source software package for simulating brash ice ship model tests. The simulation was able to capture water and ice flow around the hull qualitatively. Further work is required to validate the simulations against model test results and to obtain quantitative results on ice resistance on the ship model.

6 ACKNOWLEDGEMENT

The authors would also like to acknowledge the financial support from the Finnish-Swedish Winter Navigation Research Board through project W25-6 OreDCs.

REFERENCES

Angelidakis, V., Boschi, K., Brzeziński, K., Caulk, R. A., Chareyre, B., del Valle, C. A., Duriez, J., Gladky, A., van der Haven, D. L. H., Kozicki, J., Pekmezi, G., Scholtès, L. & Thoeni, K. (2024). YADE - An extensible framework for the interactive simulation of multiscale, multiphase, and multiphysics particulate systems. *Computer Physics Communications*, *304*. https://doi.org/10.1016/j.cpc.2024.109293

Blais, B., Barbeau, L., Bibeau, V., Gauvin, S., Geitani, T. El, Golshan, S., Kamble, R., Mikahori, G. & Chaouki, J. (2020). Lethe: An open-source parallel high-order adaptative CFD solver for incompressible flows. *SoftwareX*, *12*. https://doi.org/10.1016/j.softx.2020.100579

Chen, F. (2009). *Coupled Flow Discrete Element Method Application in Granular Porous Media using Open Source Code*. https://trace.tennessee.edu/utk_graddiss/21

Constant, M., Dubois, F., Lambrechts, J. & Legat, V. (2019). Implementation of an unresolved stabilised FEM–DEM model to solve immersed granular flows. *Computational Particle Mechanics*, *6*(2), 213–226. https://doi.org/10.1007/s40571-018-0209-4

Cundall, P. A. & Otto DL Strack. (1979). A discrete numerical model for granular assemblies. *Geotechnique*, *29*(1), 47–65.

Dadvand, P., Rossi, R. & Oñate, E. (2010). An object-oriented environment for developing finite element codes for multi-disciplinary applications. *Archives of Computational Methods in Engineering*, *17*(3), 253–297. https://doi.org/10.1007/s11831-010-9045-2

F. Moukalled, L. M. , M. D. (2016). *The finite volume method in computational fluid dynamics*.

Gong, H. (2021). *Discrete-element modelling of ship interaction with unconsolidated ice ridges: ridge resistance and failure behaviour*. Aalto University.

Hanyang Gong & Malith Prasanna. (2025). A potential application of DEM-CFD coupling methods for brash ice model testing. *Proceedings of the ASME 2025 44th International Conference on Ocean, Offshore and Arctic Engineering OMAE2025 June 22-27, 2025, Vancouver, British Columbia, Canada*.

Hopkins, M. A., Hibler III, W. D. & Flato, G. M. (1991). On the numerical simulation of the sea ice ridging process. *Journal of Geophysical Research: Oceans*, *96*(C3), 4809–4820.

Hosseini, A. & Joghataie, N. (2025). *PhasicFlowPlus* (1.0).

Kloss, C., Goniva, C., Hager, A., Amberger, S. & Pirker, S. (2012). Models, algorithms and validation for opensource DEM and CFD-DEM. *Progress in Computational Fluid Dynamics*, *12*(2–3), 140 – 152. https://doi.org/10.1504/PCFD.2012.047457

Kotouč Šourek, M., Studeník, O., Isoz, M., Kočí, P. & York, A. P. E. (2024). Viscosity prediction for dense suspensions of non-spherical particles based on CFD-DEM simulations. *Powder Technology*, *444*. https://doi.org/10.1016/j.powtec.2024.120067

Kulyakhtin, S. & Høyland, K. (2014). Distribution of ice block sizes in sails of pressure ice ridges. *The 22nd IAHR International Symposium on Ice*, 235–240.

Li, D., Shen, Z. & Wang, G. (2025). A novel hybrid CFD-DEM model for gap-graded particles with two-phase fluids. *Computers and Geotechnics*, *187*. https://doi.org/10.1016/j.compgeo.2025.107501

Lu, T. & Zou, Z. (2018). Numerical study of brash ice loads on ship hulls based on DEM-CFD. *Proceedings of the 6th European Conference on Computational Mechanics: Solids, Structures and Coupled Problems, ECCM 2018 and 7th European Conference on Computational Fluid Dynamics, ECFD 2018*, 4390–4402. https://www.scopus.com/inward/record.uri?eid=2-s2.0-85081068383&partnerID=40&md5=9f2c0487fb24f2d8e2599fa3e802436d

Luo, W, Jiang, D., Wu, T., Guo, C. & Wang, C. (2020). Numerical Study on Resistance of Ice-strengthening Bulk Carrier in Crushed Ice Channel. *Ship Building of China*, *61*(1), 41–49. https://www.scopus.com/inward/record.uri?eid=2-s2.0-85083879906&partnerID=40&md5=2431ce5d6b5a2110b326b01df03cb155

Luo, Wanzhen, Jiang, D., Wu, T., Guo, C., Wang, C., Deng, R. & Dai, S. (2020). Numerical simulation of an ice-strengthened bulk carrier in brash ice channel. *Ocean Engineering*, *196*. https://doi.org/10.1016/j.oceaneng.2019.106830

Ma, H., Zhou, L., Liu, Z., Chen, M., Xia, X. & Zhao, Y. (2022a). A review of recent development for the CFD-DEM investigations of non-spherical particles. *Powder Technology*, *412*, 117972. https://doi.org/10.1016/J.POWTEC.2022.117972

Ma, H., Zhou, L., Liu, Z., Chen, M., Xia, X. & Zhao, Y. (2022b). A review of recent development for the CFD-DEM investigations of non-spherical particles. *Powder Technology*, *412*, 117972. https://doi.org/10.1016/J.POWTEC.2022.117972

Matala, R. & Gong, H. (2021). The effect of ice fragment shape on model-scale brash ice material properties for ship model testing. *Of the 26th International Conference on Port and Ocean Engineering under Arctic Conditions*.

Morgan, D. (2016). Ice An Improved Three-Dimensional Discrete Element Model for Ice-Structure Interaction. *IAHR International Symposium 23 Rd*.

Morgan, D., Thijssen, J., Sarracino, R., Mckenna, R. & Thijssen, J. W. (2015). *Simulations of ice rubbling against conical structures using 3D DEM*. https://www.researchgate.net/publication/279178827

Norouzi, H. R. (2023). PhasicFlow: A parallel, multi-architecture open-source code for DEM simulations. *Computer Physics Communications*, *291*. https://doi.org/10.1016/j.cpc.2023.108821

Polojärvi, A. (2013). *Sea ice ridge keel punch through experiments: model experiments and numerical modeling with discrete and combined finite-discrete element methods*. Aalto University.

Polojärvi, A. (2022). Numerical model for a failure process of an ice sheet. *Computers & Structures*, *269*, 106828.

Polojärvi, A., Gong, H. & Tuhkuri, J. (2021). Comparison of full-scale and DEM simulation data on ice loads due to floe fields on a ship hull. *The 26th International Conference on Port and Ocean Engineering under Arctic Conditions*, 14–18.

Rabatel M., Labbé S. & Weiss J. (2015). Dynamics of an assembly of rigid ice floes. *J. Geophys. Res.: Oceans* , *120*, 5887–5909.

Shen, Z., Huang, D., Wang, G. & Jin, F. (2024). Numerical study of wave interaction with armour layers using the resolved CFD-DEM coupling method. *Coastal Engineering*, *187*. https://doi.org/10.1016/j.coastaleng.2023.104421

Shen, Z., Wang, G., Huang, D. & Jin, F. (2022). A resolved CFD-DEM coupling model for modeling two-phase fluids interaction with irregularly shaped particles. *Journal of Computational Physics*, *448*. https://doi.org/10.1016/j.jcp.2021.110695

SIEMENS Digital Industries. (2021). *SIMSENTER StarCCM+ Software Tutorial Guide*.

Su, Z., Xu, C., Jia, K., Cui, C. & Du, X. (2025). A novel semi-resolved CFD-DEM coupling method based on point cloud algorithm for complex fluid-particle systems. *Computer Methods in Applied Mechanics and Engineering*, *434*. https://doi.org/10.1016/j.cma.2024.117561

Syamlal, M., Rogers, W. & OBrien, T. J. (1993). *MFIX documentation theory guide*.

Tuhkuri, J. & Polojärvi, A. (2018). A review of discrete element simulation of ice–structure interaction. *Philosophical Transactions of the Royal Society A: Mathematical, Physical and Engineering Sciences*, *376*(2129), 20170335.

van den Berg M. (2016). A 3-D random lattice model of sea ice. *The Arctic Technology Conference*.

Voutilainen, J. (2023). *Computational analysis of brash ice and flow field around simplified body*. Aalto University.

Voutilainen, Juhan. (2023). *Computational analysis of brash ice and flow field around simplified body*. https://doi.org/10.04.2023

Vroegrijk, E. (2015). Validation of CFD+DEM against measured data. *Proceedings of the International Conference on Offshore Mechanics and Arctic Engineering - OMAE*, *8*. https://doi.org/10.1115/OMAE201541770

Vroegrijk, E. A. J. (2012). Application of the Discrete Element Method (DEM) on ship-ice interaction. *International Conference and Exhibition on Performance of Ships and Structures in Ice 2012, ICETECH 2012*, 128–132. https://doi.org/https://doi.org/10.5957/ICETECH-2012-120

Xie, C., Zhou, L., Ding, S., Liu, R. & Zheng, S. (2023). Experimental and numerical investigation on self-propulsion performance of polar merchant ship in brash ice channel. *Ocean Engineering*, *269*. https://doi.org/10.1016/j.oceaneng.2022.113424

You, C., Sun, T., Zhang, G., Wei, Y. & Zong, Z. (2022). Numerical study on effect of brash ice on water exit dynamics of ventilated cavitation cylinder. *Ocean Engineering*, *245*. https://doi.org/10.1016/j.oceaneng.2021.110443

Yulmetov, R., Bailey, E. & Ralph, F. (2017). A Discrete Element Model of Ice Ridge Interaction with a Conical Structure. *POAC*. https://www.researchgate.net/publication/318040270

Zhaka, V., Bridges, R., Riska, K. & Cwirzen, A. (2024). Brash ice macroporosity and piece size distribution in ship channels. *Cold Regions Science and Technology*, *217*, 104047.

Zhang, J., Zhang, Y., Shang, Y., Jin, Q. & Zhang, L. (2022). CFD-DEM based full-scale ship-ice interaction research under FSICR ice condition in restricted brash ice channel. *Cold Regions Science and Technology*, *194*. https://doi.org/10.1016/j.coldregions.2021.103454

Zou, M., Zou, Z. J., Zou, L., Chen, C. Z. & Zhang, X. S. (2024). Numerical investigations of the ice force distributions on a ship in brash ice channel using a simplified CFD-DEM solving framework. *Ocean Engineering*, *312*. https://doi.org/10.1016/j.oceaneng.2024.119103